RSC Advances

PAPER

View Article Online
View Journal | View Issue

Check for updates

Cite this: *RSC Adv.*, 2024, **14**, 14640

Influence of alkali metal ions (K^+ and Na^+) on the preparation of magnesium hydroxide hexagonal flakes

Cunjian Weng,[a] Xuewen Song, *[b] Haibin Zhu[b] and Xianping Luo *[abc]

Magnesium hydroxide ($Mg(OH)_2$), as a green halogen-free flame retardant, has attracted significant attention in the field of flame retardant composite materials. In addition to conventional indicators such as purity and whiteness, $Mg(OH)_2$ is required to take the form of regular hexagonal sheets to ensure the dispersion of composite materials. We use irregular large particles of $Mg(OH)_2$ prepared by the magnesium factory in western Qinghai as raw materials to study the influence of alkali metal ions K^+ and Na^+ mainly present in salt lakes on the physicochemical properties of $Mg(OH)_2$. The products were characterized *via* X-ray diffraction, scanning electron microscopy, automatic nitrogen physical adsorption apparatus, and other modern characterization techniques. Results show that alkali metal ions K^+ and Na^+ considerably influence the crystal surface polarity, particle size, and morphology of the prepared $Mg(OH)_2$. The mechanism analysis shows that the presence of K^+ and Na^+ alters the dissolution, recrystallization, and growth characteristics of $Mg(OH)_2$. This study provides theoretical support for the realization of high-performance $Mg(OH)_2$ using salt lake resources and demonstrates the value for promoting the large-scale industrial application of the salt lake industry.

Received 12th January 2024
Accepted 22nd April 2024

DOI: 10.1039/d4ra00305e

rsc.li/rsc-advances

Open Access Article. Published on 03 May 2024. Downloaded on 12/31/2025 2:53:18 PM.
This article is licensed under a Creative Commons Attribution-NonCommercial 3.0 Unported Licence.

1. Introduction

$Mg(OH)_2$ is nontoxic and nonpolluting and exhibits high-temperature resistance, corrosion resistance, and other excellent physical and chemical properties.[1,2] Therefore, it is widely used as an antibacterial agent in wastewater[3–5] and waste gas, for the treatment of acidic water contaminants, for fillers in the paper industry,[6] in electronic and optical devices,[7,8] and as a precursor for producing magnesium oxide[9] and new generation flame retardants.[10–15] The physical and chemical properties of $Mg(OH)_2$ products, such as the morphology, particle size, particle size distribution, dispersion, specific surface area, whiteness, and purity, play a key role in their applications. The preparation of $Mg(OH)_2$ products not only requires their high purity but also necessitates the regulation of their physical and chemical properties, such as the particle size and morphology.[16,17] Despite significant research in this area, numerous challenges remain in the actual production and preparing high-performance $Mg(OH)_2$ is still a topic of interest at present.

The hydrothermal method is commonly employed to control nucleation growth of the $Mg(OH)_2$ crystal surface by regulating its dissolution and recrystallization.[18] Currently, the use of ultrasound, microwave-assisted technology,[19] and additives,[20] among other, to regulate $Mg(OH)_2$ formation during hydrothermal reactions is a hot topic. Further, the most commonly employed method involves regulating the nucleation, crystallization, and other growth processes of $Mg(OH)_2$ using various additives.[21] Gong *et al.*[22] showed that the presence of magnesium lactate can transfer hydroxyl groups from brucite to $Mg(OH)_2$ nanoplates, thereby acting as a conveyor belt. Gómez-Villalba[23] *et al.* showed that using hydrazine hydrate as a surfactant significantly affects the physical and chemical properties, especially the morphology, of the obtained $Mg(OH)_2$ products. According to literature, inorganic alkaline crystal surface regulators, such as NaOH, can provide sufficient OH^-[24] for $Mg(OH)_2$ recrystallization and thus rearrange its structure by taking advantage of the differences in the action of different polar crystal faces and OH^-[25] to control the crystal face orientation and particle size.[26] Although there have been some studies on the use of sodium hydroxide and potassium hydroxide as crystal regulators to regulate $Mg(OH)_2$ growth, no studies exist on alkali metal ions K^+ and Na^+ as additives. Hence, herein, we conducted a study on the effects of K^+ and Na^+ on the hydrothermal synthesis of $Mg(OH)_2$ with large and irregular particles. The study provides a great reference value for the preparation of high-performance $Mg(OH)_2$.

[a]*School of Materials Science and Engineering, Xi'an University of Architecture and Technology, Xi'an 710055, China*
[b]*School of Resource Engineering, Xi'an University of Architecture and Technology, Xi'an 710055, China. E-mail: Songxwhl@163.com*
[c]*School of Resources and Environmental Engineering, Jiangxi University of Science and Technology, Ganzhou 341000, China*

© 2024 The Author(s). Published by the Royal Society of Chemistry

Open Access Article. Published on 03 May 2024. Downloaded on 12/31/2025 2:53:18 PM.
This article is licensed under a Creative Commons Attribution-NonCommercial 3.0 Unported Licence.

The influence of K^+ and Na^+ on the physical and chemical properties of prepared $Mg(OH)_2$ was studied using NaCl and KCl as crystal surface regulators and $Mg(OH)_2$ with large particles produced by the magnesium industry in western Qinghai as the raw material. Alkali metal ions K^+ and Na^+ were used to regulate the dissolution and recrystallization of $Mg(OH)_2$, related crystal growth mechanism was discussed, and low-polarity $Mg(OH)_2$ hexagonal flakes were prepared. This study has important theoretical and practical significance for the preparation of flame retardants using high-performance $Mg(OH)_2$ hexagonal flakes.

2. Material and methods

2.1. Materials

KCl and NaCl were procured from Xilong Science Co, LTD. Purified water was prepared in the laboratory. $Mg(OH)_2$ with large particles was produced by the magnesium industry in western Qinghai was used as the raw material; its morphology, particle size distribution, and crystal phase composition are shown in Fig. 1.

2.2. Experimental methods

A total of 40 g of $Mg(OH)_2$ (0.69 mol) and a certain amount of NaCl and KCl were weighed and added into a high-temperature, high-pressure reactor along with 160 mL purified water. Hydrothermal heat treatment was then performed at 500 r min^{-1} with varying additive concentration (namely KCl and NaCl concentration), reaction temperature, and reaction time. After the reaction was completed, the $Mg(OH)_2$ cake was washed using an ethanol solution to neutralize it, dried at 105 °C for 6 h, and the obtained $Mg(OH)_2$ product was sealed for subsequent characterization and analysis.

2.3. Characterization analysis test

Several analytical techniques were used to characterize the obtaine powders.

X-ray powder Diffraction. The resulting powder crystalline phases were carried out using X-ray diffraction (XRD, DX-2700BH). A Cu Kα source was used over a 2θ range of 20° to 60° and a step size of 0.02° with a dwell time of 0.05 s was applied during the analyses.

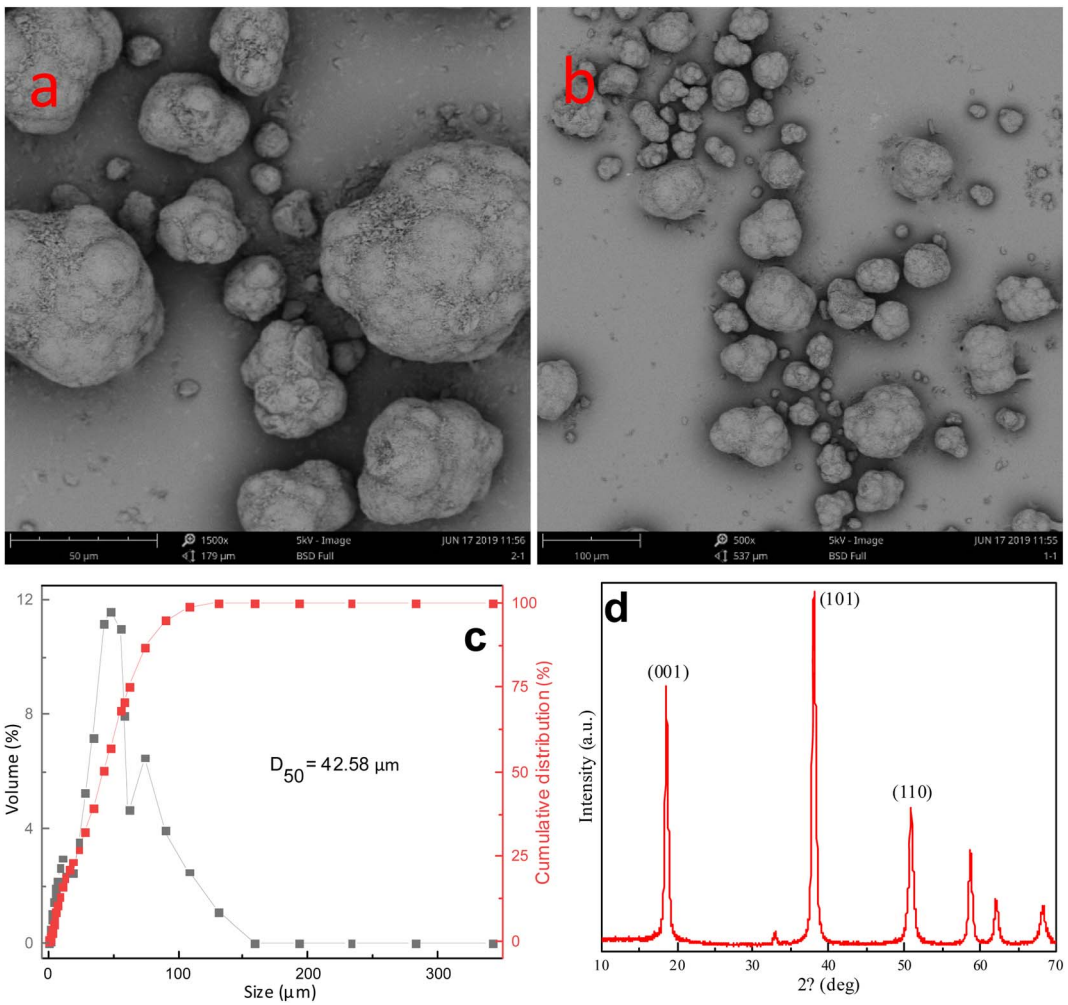

Fig. 1 Morphology, particle size distribution, and crystal phase composition of $Mg(OH)_2$ products produced by the magnesium industry in western Qinghai. ((a and b): SEM images; (c): particle size distribution and cumulative distribution; and (d): XRD pattern).

Open Access Article. Published on 03 May 2024. Downloaded on 12/31/2025 2:53:18 PM.
This article is licensed under a Creative Commons Attribution-NonCommercial 3.0 Unported Licence.

Scanning Electron Spectroscopy (SEM). The particle shape and size were analyzed by scanning electron microscopy (SEM, SU8010). The powder samples for SEM were shown and observed at a working distance of 3.5 mm and a stimulation voltage of 0.7 kV.

Dynamic light scattering (DLS). Using the dynamic light scattering method, the obtained $Mg(OH)_2$ particle, D50 size, and particle size distribution were researched by laser particle size analysis (OMCC, SCF-106A).

Brunauer–Emmett–Teller (BET). N_2 adsorption–desorption isotherms are recorded on a Micro Active for ASAP 2460 Version 2.02 at 77.300 K. N_2 adsorption–desorption isotherm (ASAP2460) is employed to analyze pore structure and surface area of $Mg(OH)_2$. Before the test, the samples are degassed overnight at 180 °C.

3. Results and discussion

The crystal phases and crystallinity of $Mg(OH)_2$ were determined *via* X-ray diffraction. Fig. 2 shows the X-ray diffraction (XRD) pattern of $Mg(OH)_2$ samples prepared at 160 °C in 6 h using different Na^+ concentrations. These XRD patterns exhibit typical diffraction peaks, which were assigned to (001), (100), (101), (102), and (110) planes of the structure of $Mg(OH)_2$. No additional XRD peaks arising from impurities were detected. As shown in Fig. 2, the strongest (*hkl*) peaks are located at 2θ values of 18.60°, 38.02°, and 50.84°, and the corresponding (*hkl*) index is as follows: (001), (101), and (102) are the main peaks of (001), (101) and (102) of $Mg(OH)_2$, respectively. The diffraction peak appears at 2θ value 58.66, corresponding to the $Mg(OH)_2$ crystal phase plane (110). The presence of Na^+ has an impact on the strength of the obtained $Mg(OH)_2$ crystal face. With the increasing content of Na^+, the strength of the (001) crystal face of the obtained $Mg(OH)_2$ product first increases and then decreases.

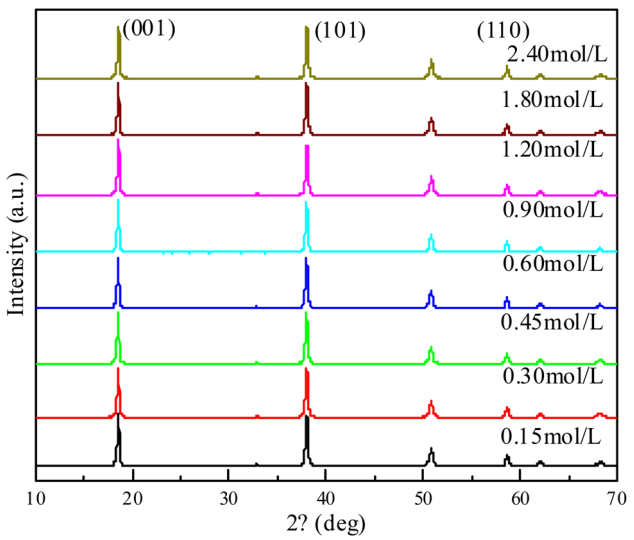

Fig. 2 $Mg(OH)_2$ products prepared using different Na^+ concentrations (reaction time: 6 h; reaction temperature: 160 °C).

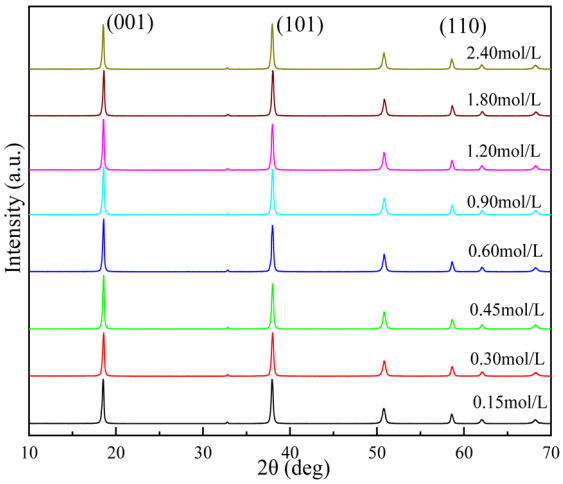

Fig. 3 $Mg(OH)_2$ products with different concentrations of K^+ (reaction time: 6 h; reaction temperature: 160 °C).

The $Mg(OH)_2$ crystal phases and crystallinity were determined by XRD. Fig. 3 shows the XRD pattern of $Mg(OH)_2$ samples prepared at a synthesis temperature of 160 °C and a synthesis time of 6 h in the presence of different concentrations of K^+. These XRD patterns exhibit typical diffraction peaks assigned to (001), (100), (101), (102), and (110) planes of the structure of $Mg(OH)_2$. No additional XRD peaks arising from impurities were detected. The strongest (*hkl*) peak detected is located at 2θ values of 18.60, 38.02, and 50.84, and the corresponding (*hkl*) index is as follows: (001), (101), and (102) are the main peaks of (001), (101) and (102) of $Mg(OH)_2$, respectively. The diffraction peak appears at 2θ value 58.66, corresponding to the $Mg(OH)_2$ crystal phase plane (110). The presence of K^+ has an impact on the strength of the obtained $Mg(OH)_2$ crystal face. With the increase in K^+ content, the crystal face of the obtained $Mg(OH)_2$ product first increases and then decreases.

Fig. 2 and 3 show that the increase in the concentration of K^+ and Na^+ leads to an increase and subsequent decrease of the intensity of (001), (101), and (110) diffraction peaks, with the intensity being the highest when the concentration of K^+ and Na^+ is 0.45 mol L^{-1}. This is attributed to less H^+ generated by hydrolysis when K^+ and Na^+ concentration is low, leading to a slower dissolution of $Mg(OH)_2$, which is not conducive to the dissolution-crystallization of Mg^{2+} on the surface of $Mg(OH)_2$, which hinders crystal growth. At high concentrations of K^+ and Na^+, hydrolysis releases more H^+ and the pH of the system is maintained at a low level, which is also not conducive to crystal growth.[27] Furthermore, due to the charge neutralization effect of anionic flocculants on $Mg(OH)_2$ and positive charge on the surface of $Mg(OH)_2$, Cl^- introduced by NaCl and KCl combines with $Mg(OH)_2$ more rapidly, further accelerating the dissolution of $Mg(OH)_2$.[28] Simultaneously, there is a higher number of impurity ions (Cl^-) in the solution, which affects the ordered crystallization of Mg^{2+} on the crystal surface of $Mg(OH)_2$ and reduces the integrity of crystal growth.

Fig. 4a shows that I_{001}/I_{101}, and I_{001}/I_{110} first increase and then decrease with increasing NaCl and KCl concentrations.

© 2024 The Author(s). Published by the Royal Society of Chemistry

Open Access Article. Published on 03 May 2024. Downloaded on 12/31/2025 2:53:18 PM.
This article is licensed under a Creative Commons Attribution-NonCommercial 3.0 Unported Licence.

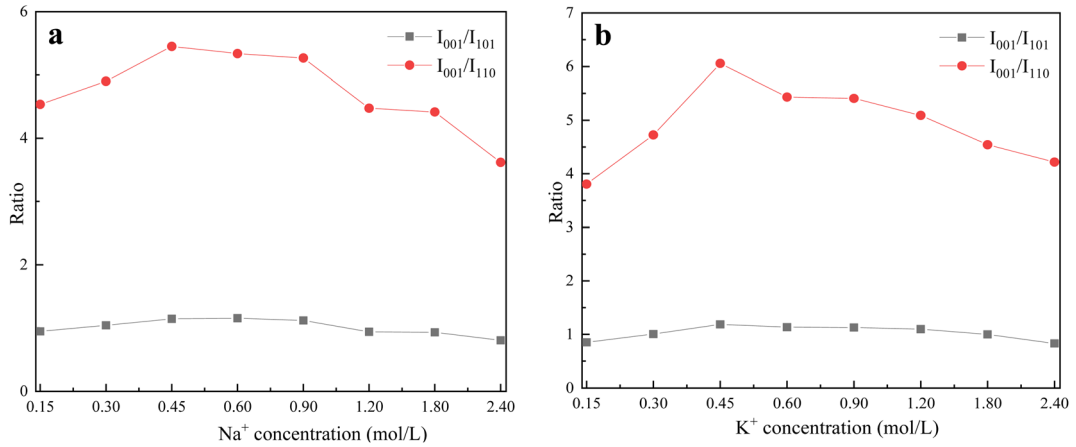

Fig. 4 XRD characteristic peak ratio of $Mg(OH)_2$ products at different Na^+ and K^+ concentrations ((a): Na^+; (b): K^+).

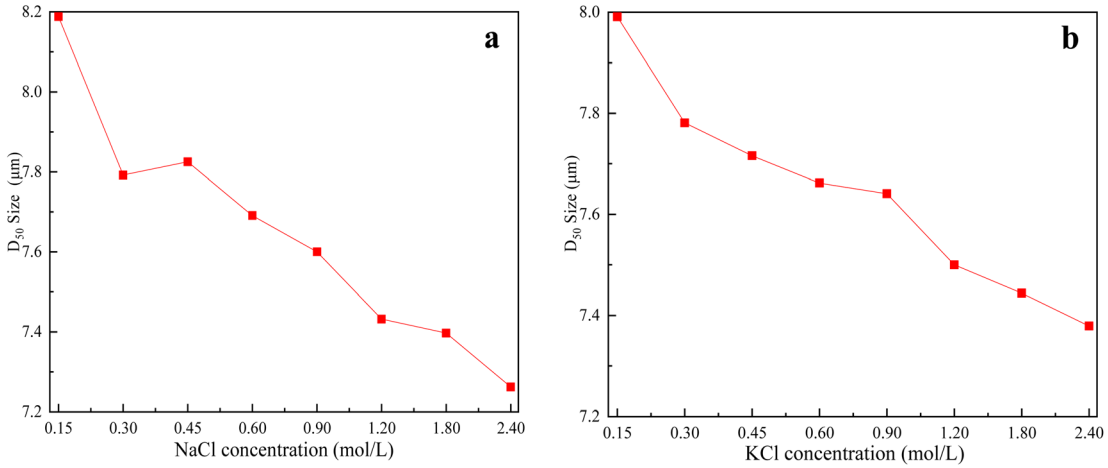

Fig. 5 D_{50} particle size variations of $Mg(OH)_2$ products at different Na^+ and K^+ concentrations ((a): Na^+; (b): K^+).

When K^+ and Na^+ concentration is 0.45 mol L^{-1}, I_{001}/I_{101} reaches its maximum. This shows that K^+ and Na^+, as crystal surface regulators, promote the selective growth of the (001) crystal surface. However, when K^+ and Na^+ concentration is low, the dissolution efficiency of $Mg(OH)_2$ decreases and the growth rate of the (001) crystal plane is lower than those of the (101) and

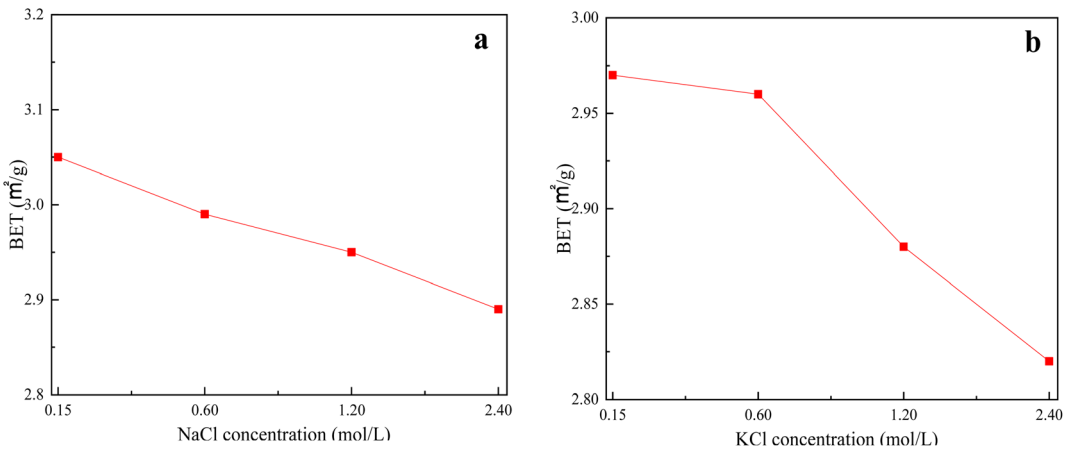

Fig. 6 BET changes of $Mg(OH)_2$ products at different Na^+ and K^+ concentrations ((a): Na^+; (b): K^+).

Open Access Article. Published on 03 May 2024. Downloaded on 12/31/2025 2:53:18 PM.
This article is licensed under a Creative Commons Attribution-NonCommercial 3.0 Unported Licence.

(110) crystal planes. When the crystal-surface-regulator concentration is high, excess Cl^- is introduced, which has a significant influence on the growth of the (001) crystal surface. We conclude that the concentrations of K^+ and Na^+, the crystal surface regulators, have a significant influence on the selective growth of the $Mg(OH)_2$ crystal surface. The increase in I_{001}/I_{101} and I_{001}/I_{110} may be attributed to the positive charge on the surface of the $Mg(OH)_2$ particles, which easily adsorb anions. As the radius of OH^- is smaller than that of the Cl^- in the precipitation system,[29] OH^- is more easily adsorbed onto the basic crystal plane of microcrystals and promotes the growth of particle edges. Thus, K^+ and Na^+ promote the growth of $Mg(OH)_2$ edges by providing Cl^- and improve the growth of the (001) crystal surface.[30]

Fig. 5 shows the variation in the particle size D_{50} of $Mg(OH)_2$ products prepared using different concentrations of NaCl and KCl. As shown in Fig. 5a, when the Na^+ concentration in the reaction system increases from 0.15 to 2.40 mol L^{-1}, the particle size of the obtained $Mg(OH)_2$ products increases from 8.18 μm dropped to 7.26 μm. Similarly, as shown in Fig. 5b, when the concentration of K^+ in the reaction system increases from 0.15 to 2.40 mol L^{-1}, the particle size of the obtained $Mg(OH)_2$ products increases from 7.99 μm dropped to 7.38 μm. We conclude that the increasing concentration of K^+ and Na^+ leads to a decrease in the particle size of the obtained $Mg(OH)_2$ products. Thus, the presence of K^+ and Na^+ has a significant effect on the dissolution and recrystallization of $Mg(OH)_2$, resulting in a continuous decrease in the particle size of the obtained products.

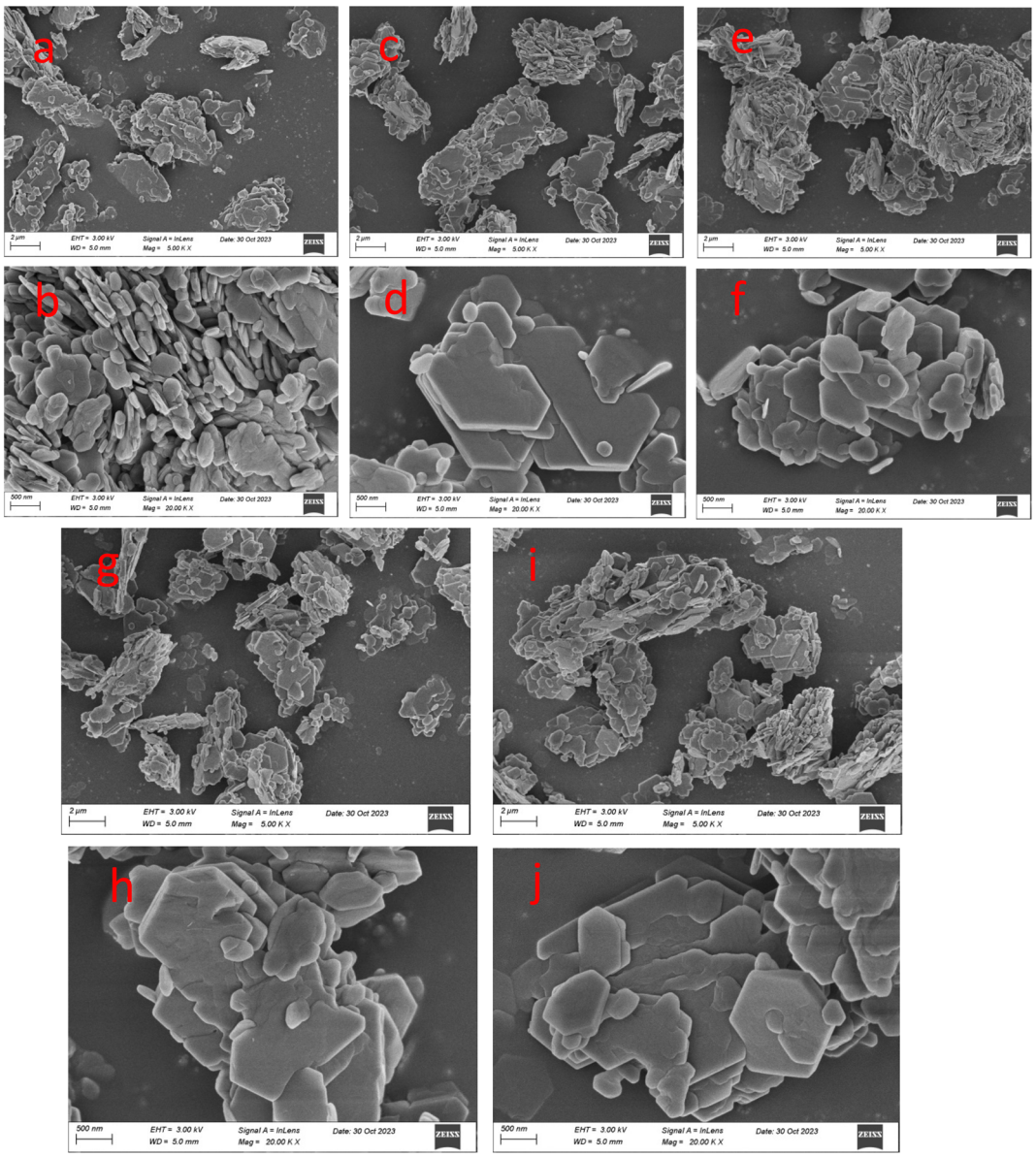

Fig. 7 Morphology of $Mg(OH)_2$ products prepared using different concentrations of Na^+ ((a and b): 0.15 mol L^{-1}; (c and d): 0.30 mol L^{-1}; (e and f): 0.60 mol L^{-1}; (g and h): 1.20 mol L^{-1}; (i, j and k): 2.40 mol L^{-1}).

© 2024 The Author(s). Published by the Royal Society of Chemistry

Open Access Article. Published on 03 May 2024. Downloaded on 12/31/2025 2:53:18 PM.
This article is licensed under a Creative Commons Attribution-NonCommercial 3.0 Unported Licence.

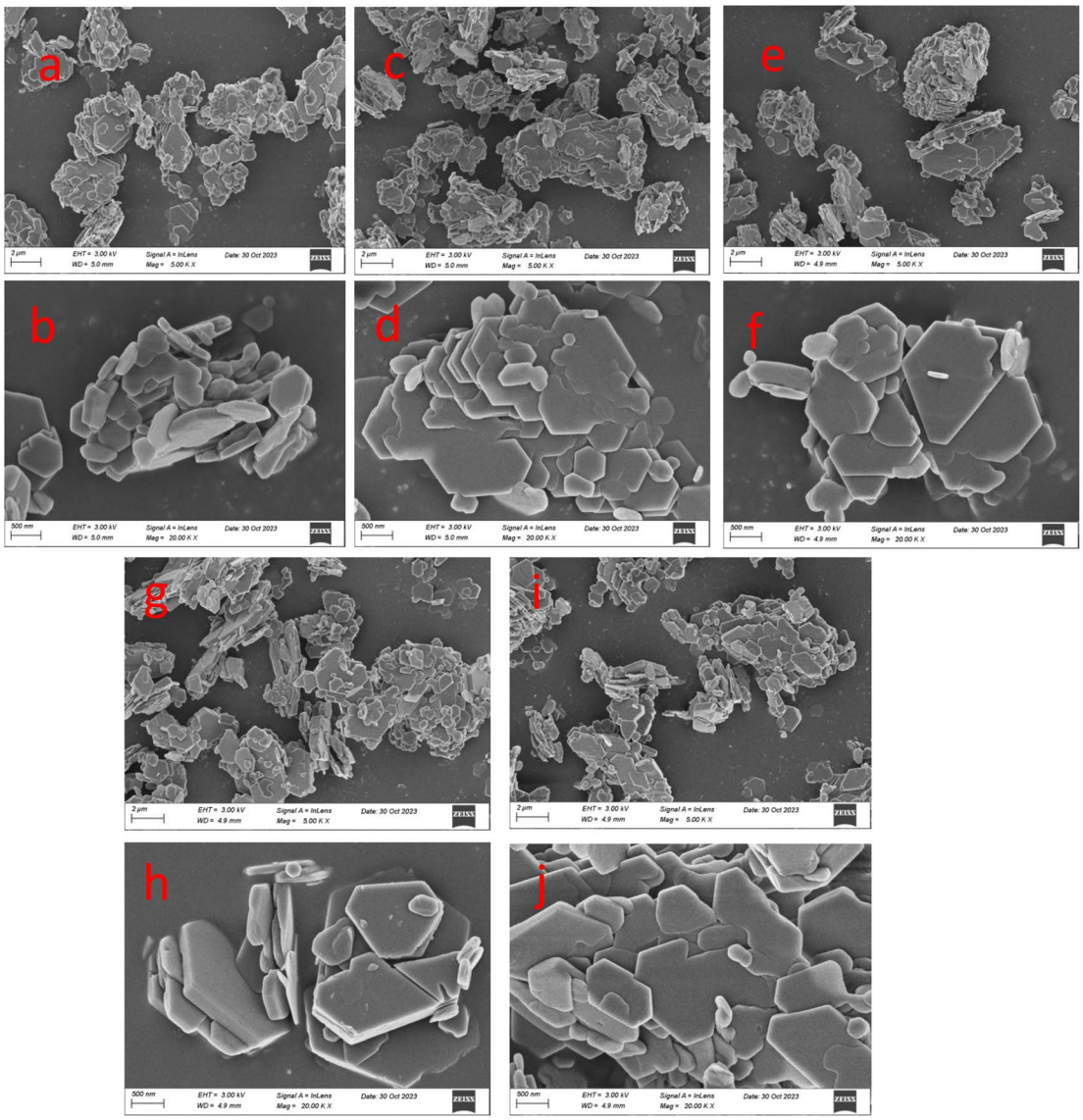

Fig. 8 Morphology of $Mg(OH)_2$ products prepared using different K^+ concentrations ((a and b): 0.15 mol L^{-1}; (c and d): 0.30 mol L^{-1}; (e and f): 0.60 mol L^{-1}; (g and h): 1.20 mol L^{-1}; (i, j and k): 2.40 mol L^{-1}).

Fig. 6 shows the BET changes of $Mg(OH)_2$ products obtained using different K^+ and Na^+ concentrations. With an increase in Na^+ concentration from 0.15 to 2.40 mol L^{-1}, the specific surface area of the obtained $Mg(OH)_2$ product decreases from 3.05 to 2.89 $m^2\ g^{-1}$ (Fig. 6a). With an increase in K^+ concentration from 0.15 to 2.40 mol L^{-1}, the specific surface area of the obtained $Mg(OH)_2$ product decreases from 2.97 to 2.82 $m^2\ g^{-1}$ (Fig. 6b). The continuous increase of alkali metal ions K^+ and Na^+ causes the specific surface area of the obtained $Mg(OH)_2$ product to decreases continuously, albeit the decrease is small. This may be attributed to the small polarity of the obtained $Mg(OH)_2$ product under these conditions, such that the presence of alkali metal ions K^+ and Na^+ has a relatively small impact on the specific surface area of $Mg(OH)_2$.

Fig. 7 and 8 show SEM images of $Mg(OH)_2$ products obtained in the presence of different concentrations of alkali metal ions K^+ and Na^+. The products obtained under these conditions are all hexagonal $Mg(OH)_2$ products. Compared with the morphology of the products obtained in Fig. 1, the morphology was subjected a significant change from irregular large particle $Mg(OH)_2$ to regular hexagonal flake $Mg(OH)_2$. This indicates that different concentrations of alkali metal ions K^+ and Na^+ play an important in the dissolution and recrystallization process of $Mg(OH)_2$, influencing the morphology of the obtained products.

4. Conclusions

Herein, we studied the influence of alkali metal ions K^+ and Na^+ as crystal surface regulators on the hydrothermal dissolution and recrystallization of $Mg(OH)_2$. The results show that the presence of K^+ and Na^+ has a significant effect on the crystal

Open Access Article. Published on 03 May 2024. Downloaded on 12/31/2025 2:53:18 PM. This article is licensed under a Creative Commons Attribution-NonCommercial 3.0 Unported Licence.

structure, polarity, and particle size of the $Mg(OH)_2$ products. Under specific hydrothermal conditions, K^+ and Na^+ play a major role in controlling the selective growth of low-polarity crystal planes of $Mg(OH)_2$. The polarity ratio of the $Mg(OH)_2$ products prepared using Na^+ decreased from the highest value of 1.19 to 0.83. When the concentration of NaCl in the reaction system increases from 0.15 to 2.40 mol L^{-1}, the particle size of the obtained $Mg(OH)_2$ products increases from 8.18 μm dropped to 7.26 μm. Similarly, an increase in the concentration of K^+ in the reaction system from 0.15 to 2.40 mol L^{-1} leads to an increase in the particle size of the obtained $Mg(OH)_2$ products from 7.99 μm dropped to 7.38 μm. K^+ and Na^+ promote the transformation of irregular large particles of $Mg(OH)_2$ products into regular hexagonal flakes under hydrothermal conditions. This study provides theoretical support for the preparation of hexagonal flakes of high-performance $Mg(OH)_2$.

Conflicts of interest

There are no conflicts to declare.

Acknowledgements

This work was partially supported by the Open Project of Salt Lake Chemical Engineering Research Complex, Qinghai University (2023-DXSSKF-01), the National Key Research and Development Program of China (2022YFC2904305) and Major Science and Technology Projects of Qinghai Province (2020-GX-A1).

References

1 C. Dong, J. Cairney, Q. Sun, *et al.*, Investigation of Mg(OH)2 nanoparticles as an antibacterial agent, *J. Nanopart. Res.*, 2010, **12**, 2101–2109.
2 W. K. Jung, H. C. Koo, K. M. Kim, *et al.*, Antibacterial activity and mechanism of action of silver ion in Staphylococcus aureus and Escherichia coli, *Appl. Environ. Microbiol.*, 2008, **74**(7), 2171–2178.
3 H. Li, S. Liu, J. Zhao, *et al.*, Removal of reactive dyes from wastewater assisted with kaolin clay by magnesium hydroxide coagulation process, *Colloids Surf., A*, 2016, **494**, 222–227.
4 K. Wang, J. Zhao, H. Li, *et al.*, Removal of cadmium (II) from aqueous solution by granular activated carbon supported Mg(OH)2, *J. Taiwan Inst. Chem. Eng.*, 2016, **61**, 287–291.
5 M. El Bouraie and A. A. Masoud, Adsorption of phosphate ions from aqueous solution by modified bentonite with magnesium hydroxide Mg(OH)2, *Appl. Clay Sci.*, 2017, **140**, 157–164.
6 R. Giorgi, C. Bozzi, L. Dei, *et al.*, Nanoparticles of Mg(OH)2: synthesis and application to paper conservation, *Langmuir*, 2005, **21**(18), 8495–8501.
7 H. Y. Zahran, S. S. Shneouda, I. S. Yahia, *et al.*, Facile and rapid synthesis of nanoplates Mg(OH)2 and MgO via Microwave technique from metal source: structural, optical and dielectric properties, *J. Sol-Gel Sci. Technol.*, 2018, **86**, 104–111.
8 S. Yousefi, B. Ghasemi, B. Tajally, *et al.*, Optical properties of MgO and Mg(OH)2 nanostructures synthesized by a chemical precipitation method using impure brine, *J. Alloys Compd.*, 2017, **711**, 521–529.
9 L. Kumari, W. Z. Li, C. H. Vannoy, *et al.*, Synthesis, characterization and optical properties of Mg(OH)2 micro-/nanostructure and its conversion to MgO, *Ceram. Int.*, 2009, **35**(8), 3355–3364.
10 X. Kong, S. Liu and J. Zhao, Flame retardancy effect of surface-modified metal hydroxides on linear low density polyethylene, *J. Cent. South Univ. Technol.*, 2008, **15**(6), 779–785.
11 A. B. Morgan and C. A. Wilkie, *Flame Retardant Polymer Nanocomposites*, John Wiley &Sons, 2007.
12 X. Hui and X. Deng, Preparation and properties of superfine Mg(OH)2 flame retardant, *Trans. Nonferrous Met. Soc. China*, 2006, **16**(2), 488–492.
13 Y. Hu and S. Li, The effects of Mg(OH)2 on flash pyrolysis of polystyrene, *J. Anal. Appl. Pyrolysis*, 2007, **78**(1), 32–39.
14 H. Balakrishnan, A. Hassan, N. A. Isitman, *et al.*, On the use of magnesium hydroxide towards halogen-free flame-retarded polyamide-6/polypropylene blends, *Polym. Degrad. Stab.*, 2012, **97**(8), 1447–1457.
15 Y. Liany, A. Tabei, M. Farsi, *et al.*, Effect of nanoclay and magnesium hydroxide on some properties of HDPE/wheat straw composites, *Fibers Polym.*, 2013, **14**(2), 304–310.
16 P. Cheng, X. LI, B. Y. PEI, *et al.*, Influence mechanism of anions on growth and morphology of Mg(OH)2 crystal, *CIESC J.*, 2017, **68**(10), 3985–3992.
17 X. Hui and X. Deng, Preparation and properties of superfine Mg(OH)2 flame retardant, *Trans. Nonferrous Met. Soc. China*, 2006, **16**(2), 488–492.
18 L. S. Gómez-Villalba, A. Sierra-Fernández, O. Milosevic, *et al.*, Atomic scale study of the dehydration/structural transformation in micro and nanostructured brucite (Mg(OH)2) particles: Influence of the hydrothermal synthesis conditions, *Adv. Powder Technol.*, 2017, **28**(1), 61–72.
19 W. Shu-Yu, H. Wen-Zhi, L. Chang, *et al.*, Characterizations and preparation of Mg(OH)2 nanocrystals through ultrasonic–hydrothermal route, *Res. Chem. Intermed.*, 2016, **42**, 4135–4145.
20 J. Du, Z. Chen, Y. L. Wu, *et al.*, The effects of solvent and microwave on the preparation of Magnesium Oxide Precursor, *Cryst. Res. Technol.*, 2014, **49**(12), 959–964.
21 B. Jia and L. Gao, Morphology transformation of nanoscale magnesium hydroxide: from nanosheets to nanodisks, *J. Am. Ceram. Soc.*, 2006, **89**(12), 3881–3884.
22 W. Gong, D. Wu, Z. Cheng, *et al.*, Direct synthesis of porous Mg(OH)2 nanoplates from natural brucite, *Mater. Res. Bull.*, 2013, **48**(3), 1333–1337.
23 L. S. Gómez-Villalba, A. Sierra-Fernández, O. Milosevic, *et al.*, Atomic scale study of the dehydration/structural transformation in micro and nanostructured brucite (Mg(OH)2) particles: Influence of the hydrothermal

© 2024 The Author(s). Published by the Royal Society of Chemistry

Open Access Article. Published on 03 May 2024. Downloaded on 12/31/2025 2:53:18 PM.
This article is licensed under a Creative Commons Attribution-NonCommercial 3.0 Unported Licence.

synthesis conditions, *Adv. Powder Technol.*, 2017, **28**(1), 61–72.

24 W. H. Lai, Y. X. Wang, Y. Wang, *et al.*, Morphology tuning of inorganic nanomaterials grown by precipitation through control of electrolytic dissociation and supersaturation, *Nat. Chem.*, 2019, **11**(8), 695–701.

25 P. Bhatt, S. Chattopadhyay, K. P. Misra, *et al.*, Effect of temporal pH variation of the reaction mixture on Mg(OH)2 morphology precipitated from an aqueous Mg(NO3)2-NaOH system, *Adv. Powder Technol.*, 2021, **32**(7), 2289–2299.

26 L. L. Jiao, P. C. Zhao, Z. Q. Liu, *et al.*, Preparation of magnesium hydroxide flame retardant from hydromagnesite and enhance the flame retardant performance of EVA, *Polymers*, 2022, **14**(8), 1567.

27 V. Berezovets, A. Kytsya, I. Zavaliy, *et al.*, Kinetics and mechanism of MgH2 hydrolysis in MgCl2 solutions, *Int. J. Hydrogen Energy*, 2021, **46**(80), 40278–40293.

28 S. L. Gou, X. Y. Nai, J. F. Xiao, *et al.*, Preparation and thermal decomposition of basic magnesium chloride whiskers, *J. Inorg. Mater.*, 2019, **34**(7), 781–785.

29 F. G. Yan, The Study on the Influence Factors of Hydration and Hydrothermal Processes to a Series of Magnesium Compound products, PhD thesis, East China Normal University, Shanghai, 2019.

30 Y. W. Cao, Y. Liu, H. M. Kong, *et al.*, Selective growth control and mechanism analysis of Mg(OH)2 low-polarity crystal surfaces, *Fine Chem.*, 2022, **39**(10), 2035–2043.